

# Capillary Flow Properties of Thermotropic Hydroxypropylcelluloses

MITSUYOSHI FUJIYAMA, *Polymer Development Laboratory,  
Tokuyama Soda Co., Ltd., Tokuyama-shi, Yamaguchi-ken 745, Japan*

## Synopsis

The influences of molecular weight, temperature, and shear rate on the capillary flow properties of thermotropic hydroxypropylcelluloses have been studied. The crystalline/liquid crystalline transition temperature and the temperatures at which the liquid crystalline/isotropic transition begins and ends are higher as the molecular weight is higher. The flow curves show yield stresses and, contrary to general thermoplastic resins, the slope of  $\log(\text{viscosity})$ – $\log(\text{shear rate})$  curve decreases as the shear rate increases. This tendency is more notable as the molecular weight is higher. The temperature change of the viscosity shows a minimum and the minimum moves to a higher temperature with increasing shear rate. The moving rate is higher as the molecular weight is higher. This is because the molecular orientation of the isotropic phase increases with increasing shear rate. Contrary to general thermoplastic resins, the molecular weight dependence of the viscosity increases with increasing shear rate. The yield stress is higher as the molecular weight is higher and shows a minimum at 200–210°C. The molecular weight dependence of the entrance pressure loss is higher than that of the viscosity. The end correction coefficients of the hydroxypropylcelluloses are very much higher than those of general thermoplastic resins: They exceed 50 in some cases. The temperature change of the end correction coefficient shows a maximum and the temperature at the maximum is higher as the molecular weight is higher. The die swell ratio shows a minimum at 180–220°C at low shear rates and the minimum swell ratio is lower than unity in some cases. The die swell ratio is higher as the molecular weight is increased.

## INTRODUCTION

Thermotropic liquid crystalline polymers have received attention as self-reinforced plastics since, because of their ease of molecular orientation, high strength and high modulus articles can be obtained by use of usual processing methods such as extrusion, injection molding, and melt spinning. In order to study the processability of thermotropic liquid crystalline polymers, their rheological properties have been actively investigated.<sup>1,2</sup>

Shimamura et al.<sup>3</sup> have first shown that a hydroxypropylcellulose (HPC) shows a thermotropic mesophase. Suto et al.<sup>4</sup> measured the rheological properties of cellulose derivatives including HPC in the molten state. They reported that an HPC with a weight-average molecular weight of 60,000 showed behaviors similar to those of isotropic polymer melts at temperatures above 200°C and behaviors characteristic of mesophase: existence of a yield stress, long relaxation time, and too small die swell at temperatures below 190°C. Chen et al.<sup>5</sup> studied the elongational flow properties on the same cellulose derivatives as used by Suto et al.<sup>4</sup> They reported that the HPC showed deformation softening behaviors: hence a draw resonance occurred at a low drawdown ratio and no vortex was formed at the inlet region of a die. Horio et al.<sup>6</sup> measured the steady state flow properties and the dynamic

viscoelastic properties of an HPC with a weight-average molecular weight of 104,300 in the molten state. As the result, the steady state viscosity  $\eta$  showed a minimum at 175°C and a maximum at 190°C, and the decreases of the dynamic viscoelastic functions ( $\eta'$ ,  $G'$ ,  $G''$ ) with temperature showed downward breaks at 190°C. They concluded from the experimental results that the HPC shows a mesophase in the temperature range of 130–175°C, that an isotropic phase begins to appear at 175°C and becomes notable at 190°C, and that it becomes completely isotropic in the temperature range of 225–250°C.

This study is concerned with the capillary flow properties of thermotropic HPCs. The influences of molecular weight, temperature, and shear rate on the viscosity  $\eta$ , the yield stress  $\tau_y$ , the entrance pressure loss  $P_0$ , the end correction coefficient  $\nu$ , and the die swell ratio  $D/D_0$  have been studied in detail.

Although Suto et al.<sup>7,8</sup> closely studied the influences of solvent, concentration, and shear rate on the capillary flow properties of lyotropic HPCs, there is only a brief study of Suto et al.<sup>4</sup> on the capillary flow properties of a thermotropic HPC.

## EXPERIMENTAL

### Sample

Three kinds of HPCs, HPC-H, HPC-M, and HPC-L, which were manufactured by Nihon Soda Co., Ltd. were used. The properties of the HPC samples are shown in Table I. Each measurement was done on the sample dried under vacuum at 60°C for 24 h.

### Measurement

#### *Polarizing Microscopy*

The powder sample was put between two glass plates, melted on a hot plate at 200°C, pressed gently, cooled slowly in air, and a sheet about 0.1 mm thick was molded. It was heated on a Metler hot stage at a rate of 5°C/min and the

TABLE I  
Properties of Samples

Name	Sample			Flow test $T_f^b$ (°C)	Polarized microscopy		DSC $T_p^e$ (°C)
	Solution viscosity <sup>a</sup> (cps)	$\bar{M}_w$ ( $\times 10^4$ )	Hydroxypropyl group content (%)		$T_b^c$ (°C)	$T_e^d$ (°C)	
HPC-H	2500	34	63.5	150	205	240	216
HPC-M	287	13.7	63.3	140	190	225	214
HPC-L	8.9	6.6	63.0	130	180	215	203

<sup>a</sup> 2 wt % solution in water.

<sup>b</sup> Temperature at which flow begins under apparent shear stress of  $2.45 \times 10^6$  dyn/cm<sup>2</sup>.

<sup>c</sup> Temperature at which transmitted light intensity under crossed polars begins to decrease.

<sup>d</sup> Temperature at which transmitted light intensity under crossed polars becomes zero.

<sup>e</sup> Peak temperature of heating thermogram.

morphology and the transmitted light intensity  $I/I_0$  were measured with a polarizing microscope (Olympus PM-6) under crossed polars.

### *Differential Scanning Calorimetry*

The melting behavior was measured on about 25 mg sample with a differential scanning calorimeter, Perkin-Elmer BI at a heating rate of  $10^\circ\text{C}/\text{min}$ .

### *Capillary Rheometry*

The capillary flow properties were measured with a Koka Flow Tester, a plunger extrusion-type rheometer produced by Shimazu Seisakusho Co., Ltd. using three straight dies with capillary diameter  $2R = 0.5$  mm, capillary length  $L = 1.0, 2.5$ , and  $5.0$  mm, and  $L/R = 4, 10$ , and  $20$ .

First, as preliminary experiment, the flow-beginning temperature,  $T_f$ , was measured by the temperature-rising method at a heating rate of  $3^\circ\text{C}/\text{min}$  with a die of  $L/R = 20$  under a pressure of  $100 \text{ kg}/\text{cm}^2$  (an apparent shear stress of  $2.45 \times 10^6 \text{ dyn}/\text{cm}^2$ ). The results are shown in Table I.

Next, the capillary flow properties were measured by the constant temperature method. After preheating under a pressure of  $10 \text{ kg}/\text{cm}^2$  for 10 min, the relation between pressure  $P$  and volumetric flow rate  $Q$  was measured. After the extrudate was solidified, its diameter  $D$  at a place 5 cm far from the front was measured with a micrometer and the ratio  $D/D_0$ , where  $D_0$  is the diameter of the capillary, was used as a measure of the die swell.

In the capillary flow, the apparent shear stress  $\tau'_w$  and the apparent shear rate  $\dot{\gamma}'_w$  at the wall of the capillary are given by eqs. (1) and (2), respectively,

$$\tau'_w = PR/2L \quad (1)$$

$$\dot{\gamma}'_w = 4Q/\pi R^3 \quad (2)$$

In the case of the Koka flow tester, in which fluid flows from the reservoir with a relatively large diameter into the die with a relatively small diameter, a pressure loss due to the contraction of the flow at the die inlet  $P_0$  occurs. In such a case the effective shear stress  $\tau$  is given by the following equations<sup>9</sup>:

$$\tau = (P - P_0)R/2L \quad (3)$$

$$= PR/2(L + \nu R) \quad (3')$$

where  $\nu R$  is the capillary length corresponding to  $P_0$  and  $\nu$  is the end correction coefficient.

When flow is non-Newtonian, a correction is needed for the shear rate. The true shear rate  $\dot{\gamma}$  is given by<sup>10</sup>

$$\dot{\gamma} = \frac{\dot{\gamma}'_w}{4} \left\{ 3 + \frac{d \log \dot{\gamma}'_w}{d \log \tau} \right\} \quad (4)$$

The shear viscosity  $\eta$  is given by

$$\eta = \tau/\dot{\gamma} \quad (5)$$

## RESULTS AND DISCUSSION

### Measurement of Temperature Changes of Morphology and Transmitted Light Intensity with Polarizing Microscope

The temperature change of the morphology is shown in Figure 1. Although clear textures are observed at low temperatures, they rapidly become dark from around 220°C for HPC-H, from around 210°C for HPC-M, and from around 200°C for HPC-L.

The temperature changes of the transmitted light intensity  $I/I_0$  are shown in Figure 2. It begins to drop at around 205°C for HPC-H, at around 190°C for HPC-M, and at around 180°C for HPC-L, and becomes zero at around 240°C for HPC-H, at around 225°C for HPC-M, and at around 215°C for HPC-L. These values are shown in Table I.

### Differential Scanning Calorimetry

DSC heating thermograms are shown in Figure 3. An endotherm begins at around 160°C and ends at around 240°C. A peak is observed at 216°C for HPC-H, at 214°C for HPC-M, and at 203°C for HPC-L. The peak temperatures  $T_p$  are shown in Table I.

From these experimental results, it is presumed that the states of the HPCs used in this experiment change as shown in Table II. Each transition temperature is higher as the molecular weight is higher and the difference of each transition temperature among samples is about 10°C. Seurin et al.<sup>11</sup> reported that the liquid crystalline/isotropic transition temperature (corresponding to  $T_e$  of the present experiment) of HPC increased with increasing molecular weight.

### Capillary Flow Properties

An example of the relation between apparent shear rate  $\dot{\gamma}'_w$  and pressure  $P$  is shown for HPC-M measured at 200°C in Figure 4. An example of the Bagley plots made by use of Figure 4 is shown in Figure 5. Fine Bagley plots were obtained for all the samples at all the temperatures. In Figure 6 are shown the apparent flow curves ( $\dot{\gamma}'_w - \tau'_w$ ) obtained with dies of  $L/R = 4, 10$ , and  $20$ , the flow curve ( $\dot{\gamma}'_w - \tau$ ) obtained by correcting the apparent shear stress  $\tau'_w$  to the effective shear stress  $\tau$  through eq. (3) by use of the entrance pressure loss  $P_0$  obtained as the intercept of the  $P$ -axis in the Bagley plot, and the true flow curve ( $\dot{\gamma} - \tau$ ) obtained by correcting the apparent shear rate  $\dot{\gamma}'_w$  to the true shear rate  $\dot{\gamma}$  through eq. (4). Although, due to the entrance pressure loss, the  $\dot{\gamma}'_w - \tau'_w$  curve is located at higher shear stress side as  $L/R$  is lower, each flow curve with different  $L/R$  unites into one curve independent of  $L/R$  when  $\tau'_w$  is corrected to  $\tau$ .

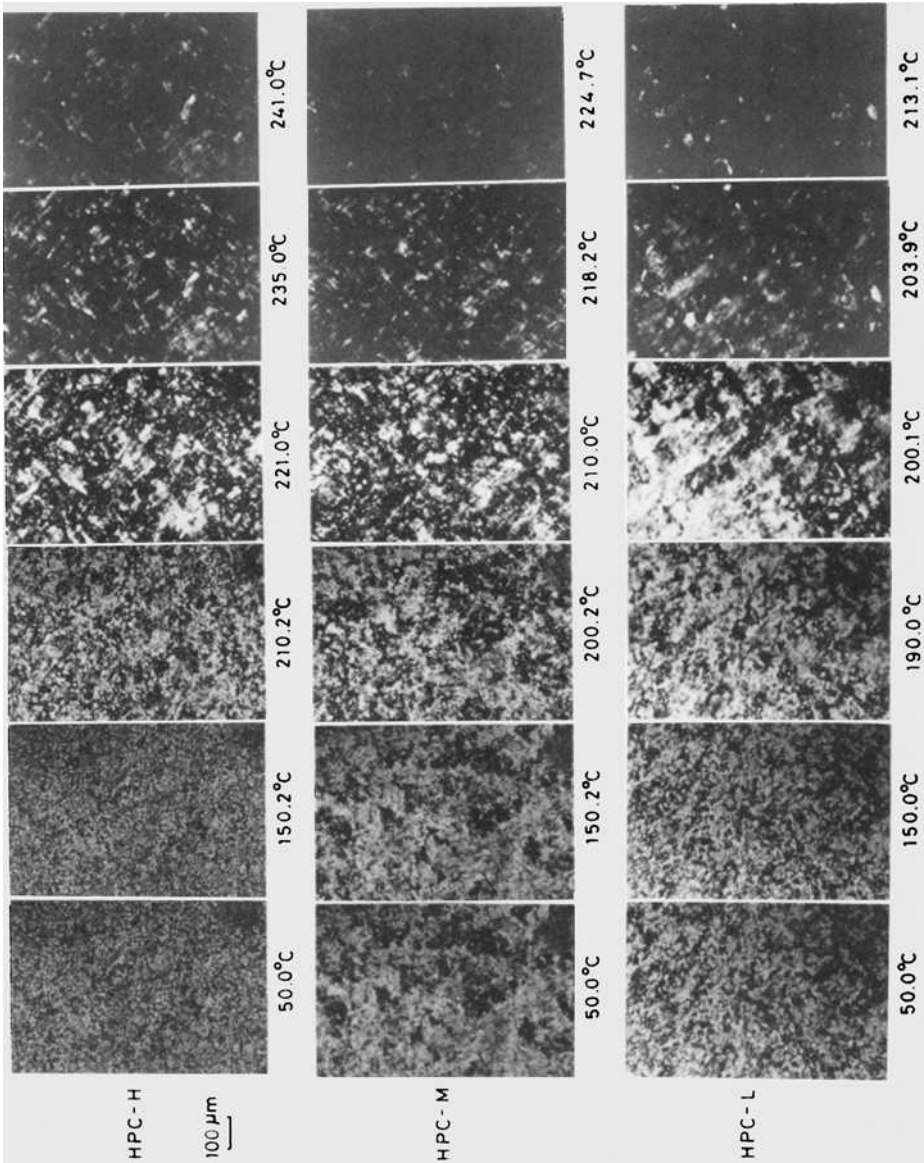


Fig. 1. Variations of polarizing micrograph with temperature.

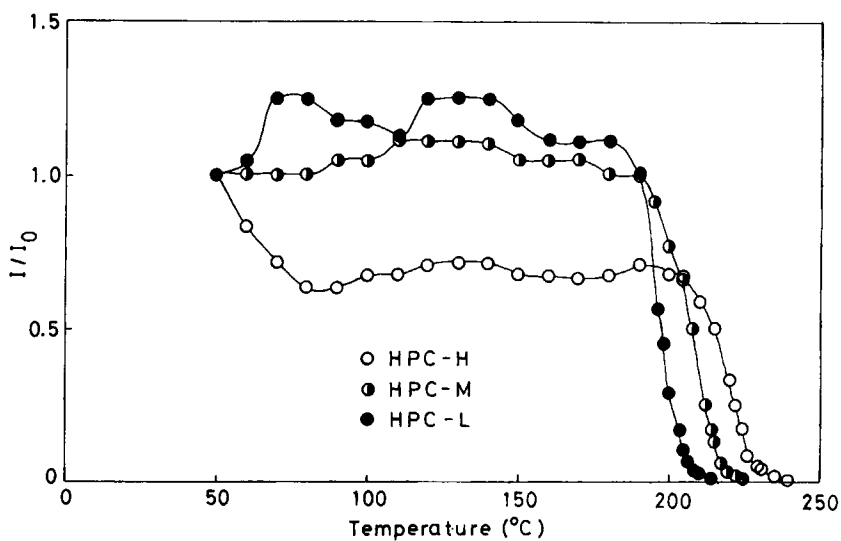


Fig. 2. Variations of transmitted light intensity under crossed polars with temperature.

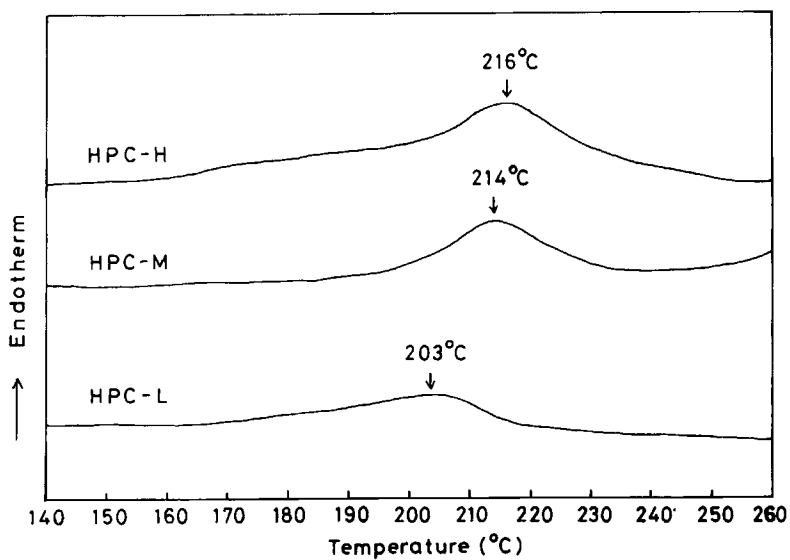


Fig. 3. DSC heating thermograms.

TABLE II  
State Change of HPCs

Sample	Crystalline	Liquid crystalline	Biphasic	Isotropic
HPC-H	-150°C	150-205°C	205-240°C	240°C-
HPC-M	-140°C	140-190°C	190-225°C	225°C-
HPC-L	-130°C	130-180°C	180-215°C	215°C-

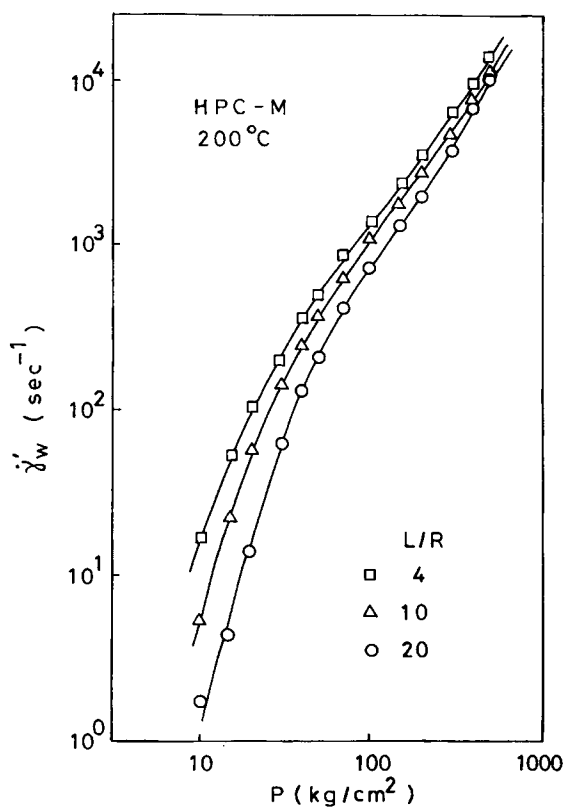


Fig. 4. An example of the relation between apparent shear rate  $\dot{\gamma}'_w$  and pressure  $P$ .

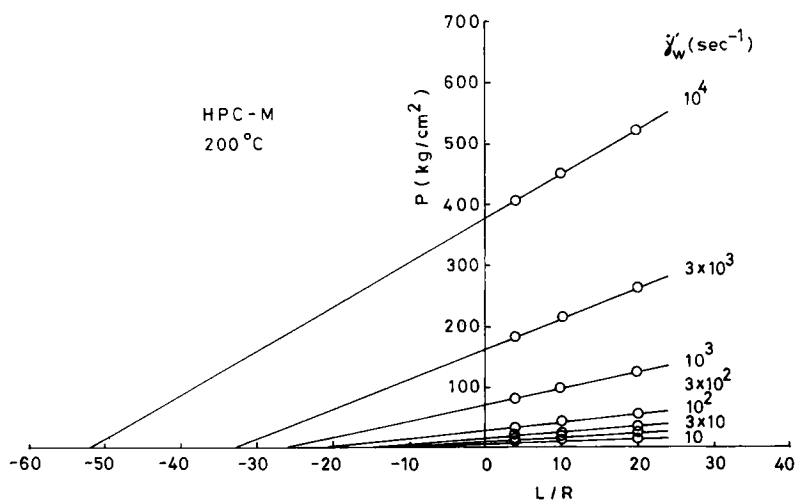


Fig. 5. Bagley plots.

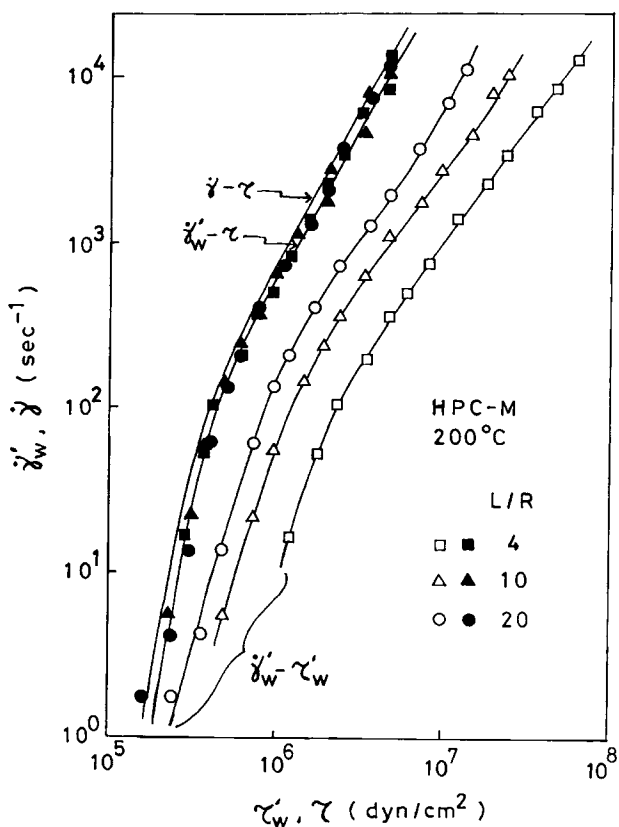


Fig. 6. Flow curves corrected at each stage.

### Viscosity

The  $\eta$ - $\dot{\gamma}$  curves calculated from the  $\dot{\gamma}$ - $\tau$  curves using eq. (5) are shown in Figure 7. All the  $\eta$ - $\dot{\gamma}$  curves continue to increase at low shear rates, which indicates the existence of the yield stress. Although Suto et al.<sup>4</sup> reported that an HPC with a weight-average molecular weight of 60,000 approached the Newtonian flow at low shear rates at temperatures above 200°C, all the HPCs used in this experiment do not approach the Newtonian flow at low shear rates at all the temperatures. The slope of the flow curve at low shear rates is rather higher at higher temperatures. Contrary to general thermoplastic resins, the slope of the flow curve decreases with increasing shear rate and it is presumed that the flow curves at high shear rates approach the region II in the general flow curve of liquid crystals which has been proposed by Onogi and Asada.<sup>12</sup> This tendency is more notable as the molecular weight is increased. Furthermore, the phenomenon characteristic of liquid crystalline polymers that the viscosity increases with increasing temperature appears at low shear rates. Such a phenomenon has already been observed for thermotropic HPCs by Suto et al.,<sup>4</sup> Chen et al.,<sup>5</sup> and Horio et al.<sup>6</sup> This is considered to be caused by a balance between the decrease of the viscosity of the liquid crystalline phase with increasing temperature and the increase of



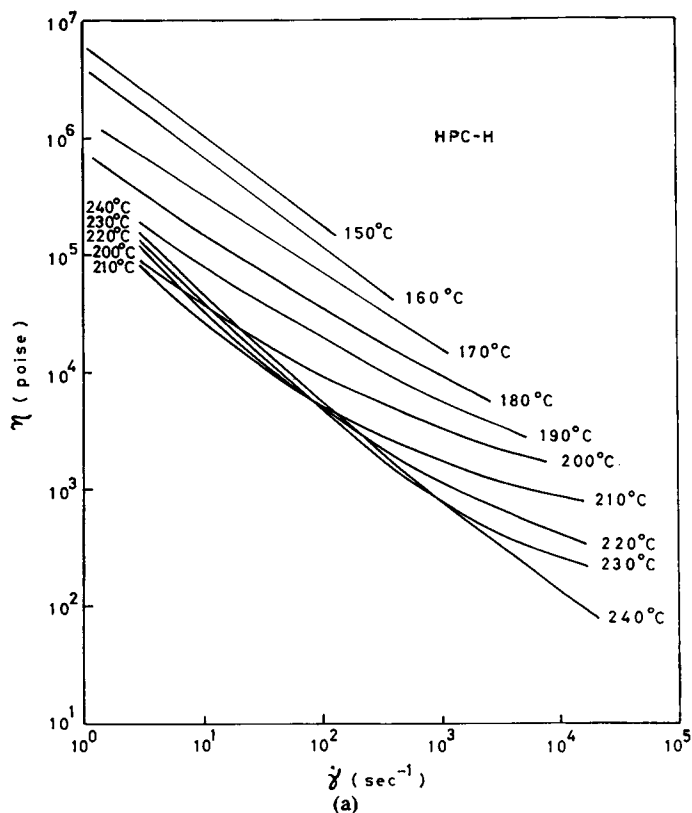


Fig. 7. True flow curves: (a) HPC-H; (b) HPC-M; (c) HPC-L.

the viscosity due to the transition from the liquid crystalline phase to the isotropic phase, which has a higher viscosity than the liquid crystalline phase at the temperature.

Figure 8 shows the temperature changes of the viscosity using the shear rate  $\dot{\gamma}$  as a parameter. The temperature at which the viscosity shows a minimum moves toward higher temperature with increasing shear rate. This moving rate is higher as the molecular weight is higher and the temperature does not move for HPC-L. The cause of the move of the temperature toward higher temperature with increasing shear rate is assumed to be as follows: The liquid crystalline phase shows low viscosity since its molecular chains are readily oriented under shear stress. Meanwhile, at high shear rates, the isotropic phase also shows low viscosity due to high degree of molecular orientation. As a result, the difference between the viscosity of the liquid crystalline phase and that of the isotropic phase becomes small at high shear rates. It is considered that the degree of molecular orientation in the isotropic phase at high shear rates increases with increasing molecular weight because of chain entanglement and that the degree of molecular orientation in the liquid crystalline phase does not depend so much on the molecular weight because of no chain entanglement. Then the degree of decrease of the viscosity difference between the liquid crystalline and the isotropic phases with increasing shear rate is higher as the molecular weight is increased.

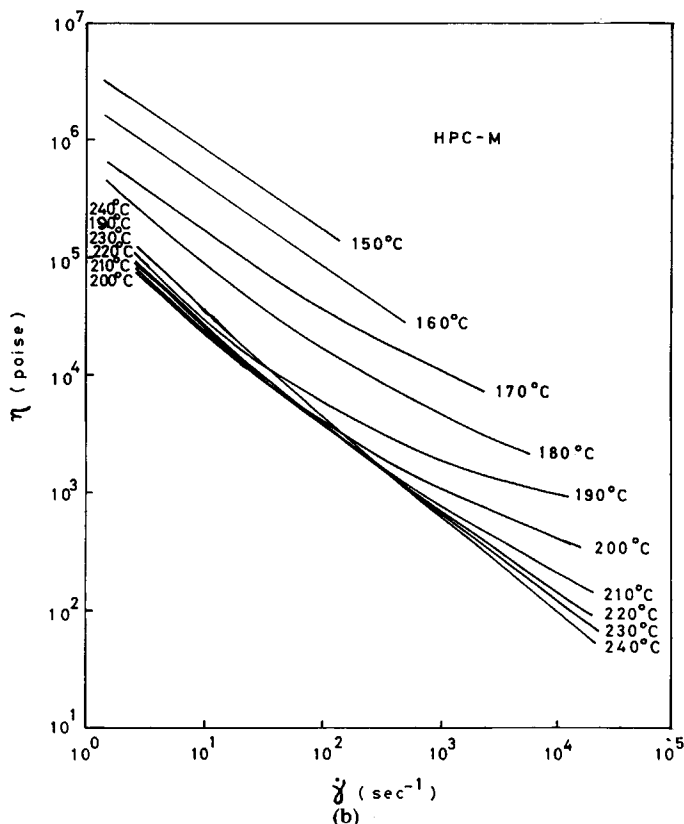


Fig. 7. (Continued from the previous page.)

Figure 9 shows a comparison of the temperature change of the viscosity among samples. The viscosity is higher as the molecular weight is higher at all the shear rates at all the temperatures. The double logarithmic plot of the viscosity  $\eta$  at a constant temperature at a constant shear rate vs. weight-average molecular weight  $\bar{M}_w$  is not linear. A characteristic matter is that, contrary to general thermoplastic resins, the dependence of the viscosity on the molecular weight becomes notable with increasing shear rate. This is assumed to be due to the fact that, contrary to general thermoplastic resins, the flow curve approaches the Newtonian flow with increasing shear rate as shown in Figure 7. Furthermore, although the temperature at which the viscosity shows a minimum is 200–210°C and does not depend on the molecular weight at low shear rates, it moves toward higher temperature with increasing molecular weight at high shear rates. This is due to the molecular orientation in the isotropic phase as described previously.

### Yield Stress

Figure 10 shows the temperature changes of the yield stress  $\tau_y$ , which was obtained from the Casson plot ( $\tau^{1/2}$  vs.  $\dot{\gamma}^{1/2}$ ).<sup>13</sup> Since the flow curve ( $\log \dot{\gamma} - \log \tau$ ) is linear and the Casson plot is not linear at temperatures below 170°C for HPC-H and at temperatures below 160°C for HPC-M,  $\tau_y$

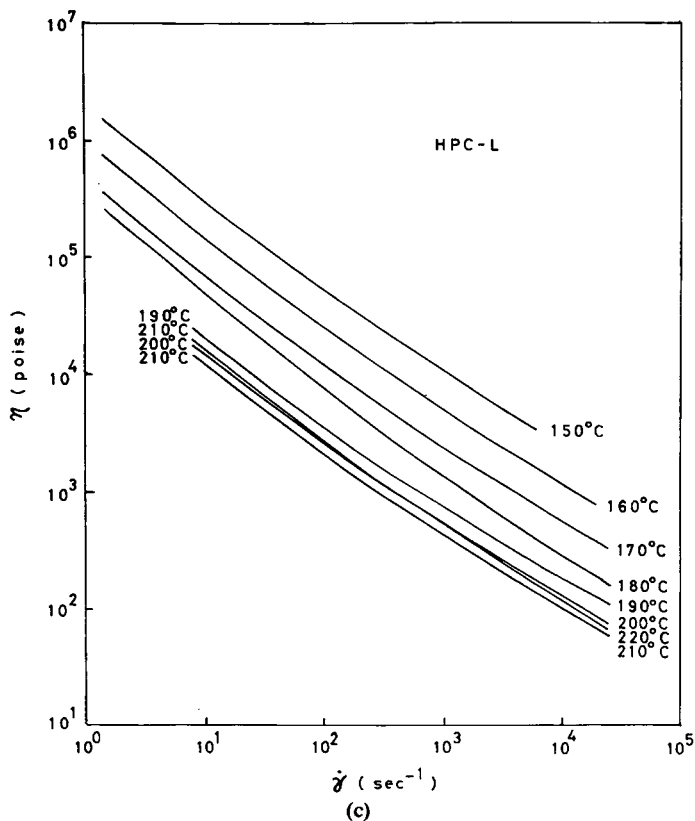
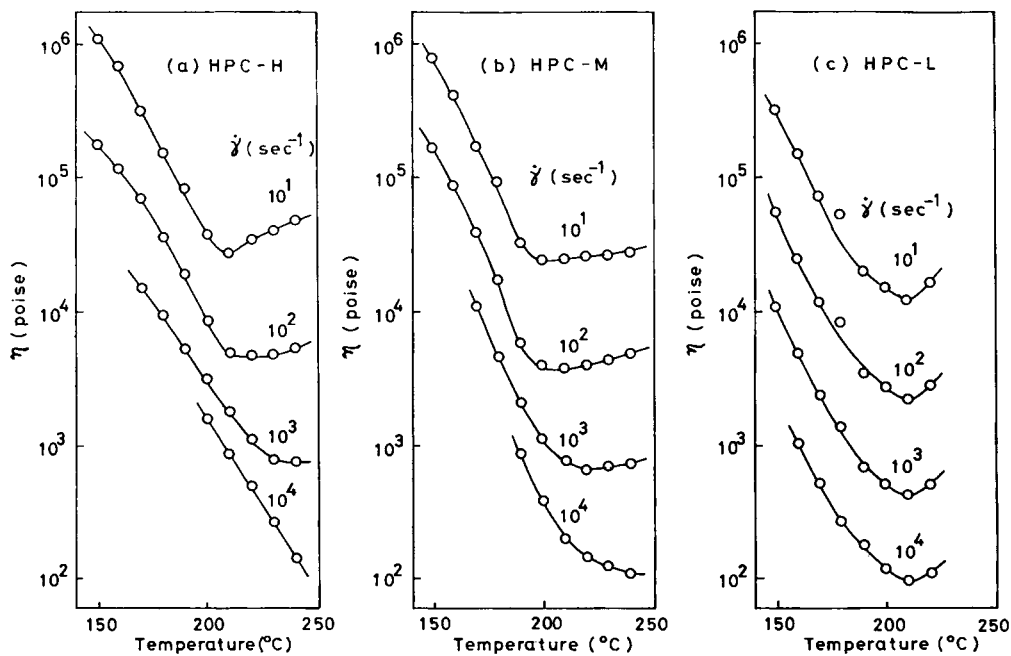


Fig. 7. (Continued from the previous page.)

Fig. 8. Temperature changes of viscosity  $\eta$ : (a) HPC-H; (b) HPC-M; (c) HPC-L.

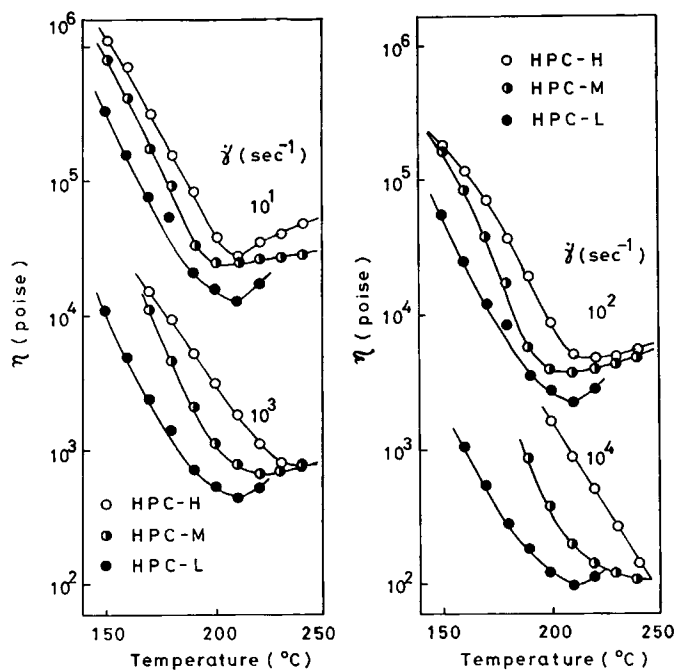


Fig. 9. Comparison of temperature change of viscosity  $\eta$  among samples.

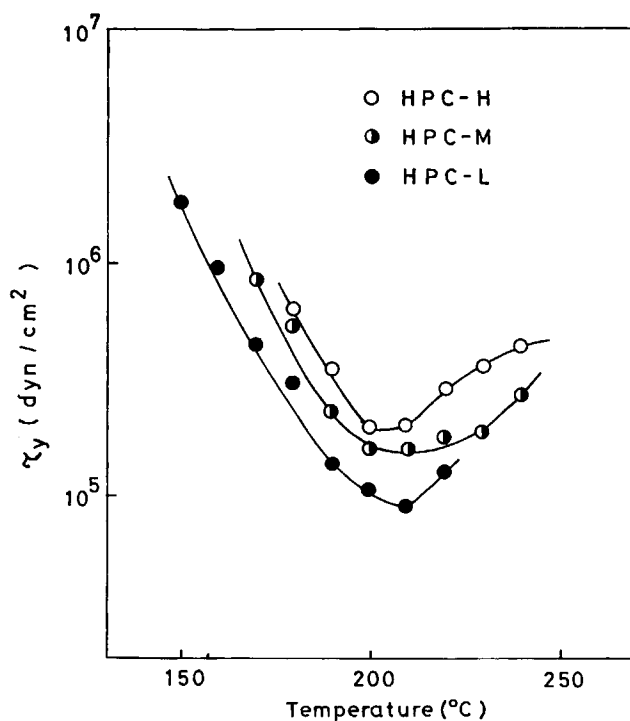


Fig. 10. Temperature changes of yield stress  $\tau_y$ .

could not be obtained in these cases. The temperature changes of  $\tau_y$  are similar to those of the viscosity at low shear rates and show minima at 200–210°C.  $\tau_y$  is higher as the molecular weight is higher. Similar to the results of Sugiyama et al.<sup>14</sup> for thermotropic copolyesters, plots of  $\log \dot{\gamma}$  versus  $\log(\tau - \tau_y)$  are linear, and HPCs behave as a nonlinear Bingham liquid.

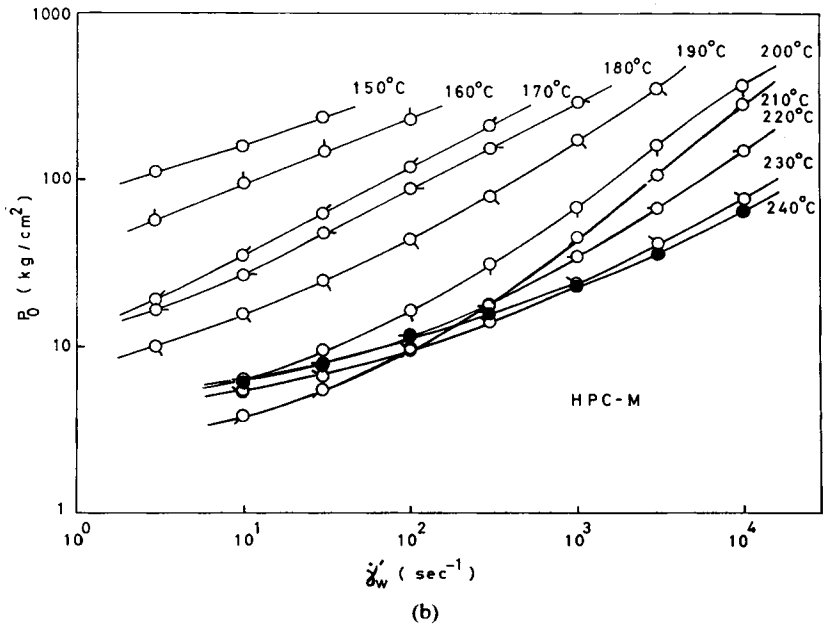
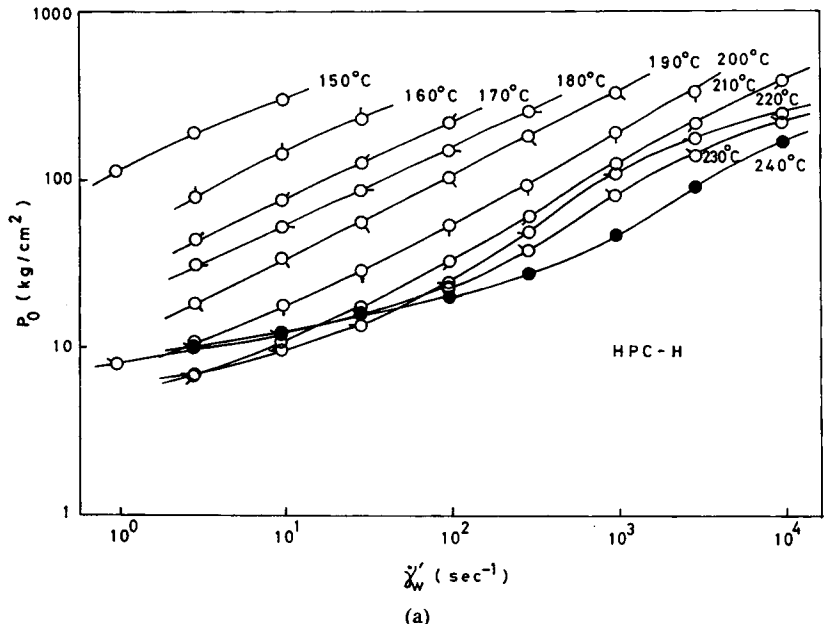


Fig. 11. Variations of entrance pressure loss  $P_0$  with apparent shear rate: (a) HPC-H; (b) HPC-M; (c) HPC-L.

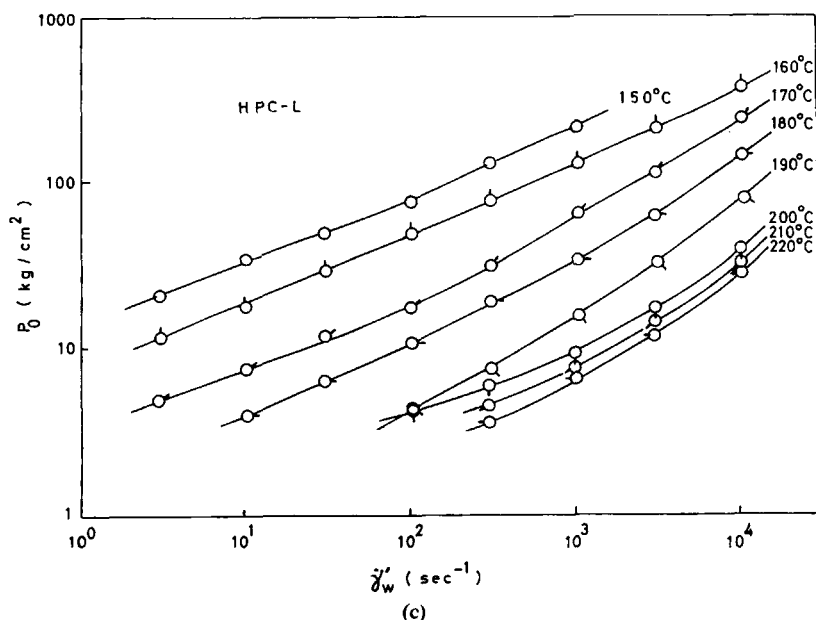
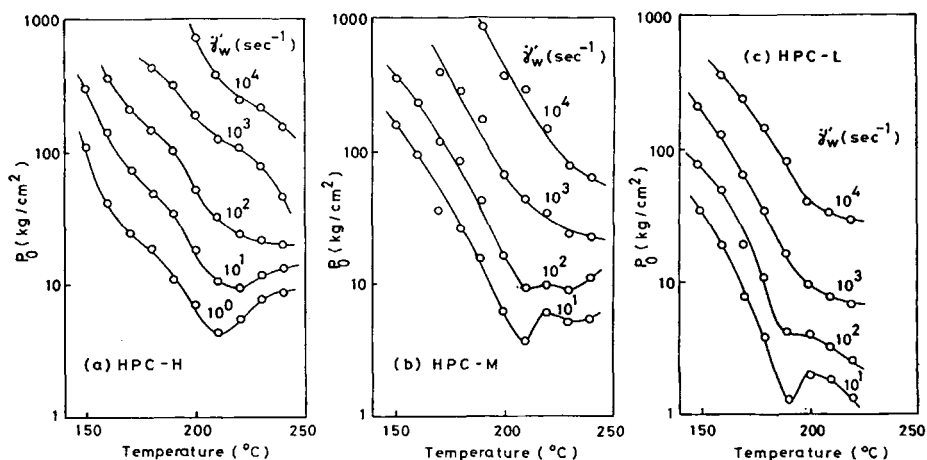


Fig. 11. (Continued from the previous page.)

### Entrance Pressure Loss

Figure 11 shows the variations, with the apparent shear rate  $\dot{\gamma}_w'$ , of the entrance pressure loss  $P_0$  which was obtained as the intercept of the  $P$ -axis in the Bagley plot.  $P_0$  tends to increase with increasing shear rate and decrease with increasing temperature. An inversion occurs at high temperatures at low shear rates as in the case of viscosity  $\eta$ .

Figure 12 shows the temperature changes of  $P_0$  using the apparent shear rate as a parameter.  $P_0$  shows a minimum and a maximum at low shear rates and the temperatures at the minimum and the maximum are higher as the molecular weight is higher.

Fig. 12. Temperature change of entrance pressure loss  $P_0$ : (a) HPC-H; (b) HPC-M; (c) HPC-L.

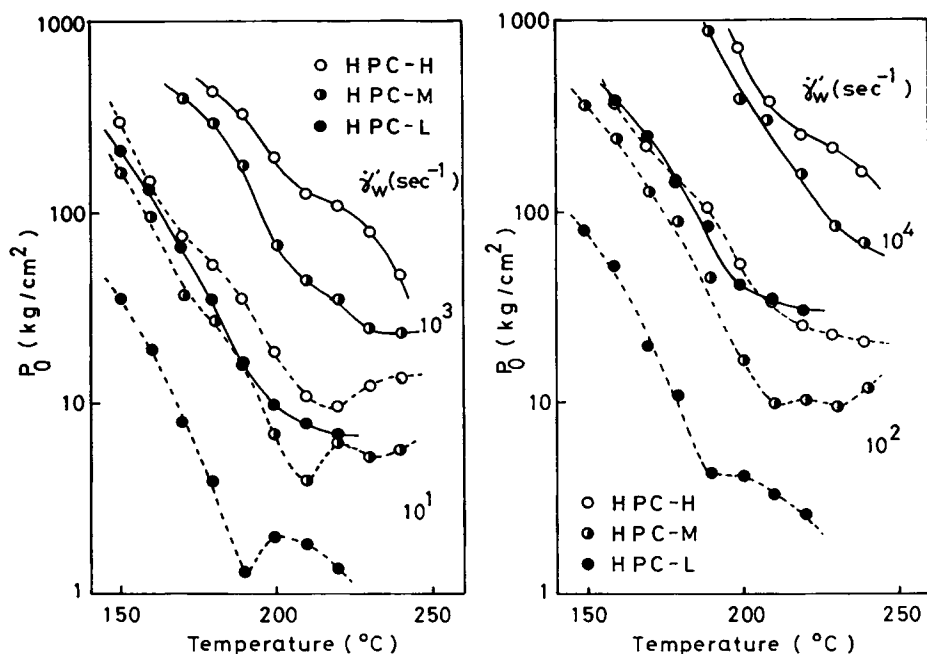


Fig. 13. Comparison of temperature change of entrance pressure loss  $P_0$  among samples.

Figure 13 shows a comparison of the temperature change of  $P_0$  among samples.  $P_0$  is higher as the molecular weight is higher at all the shear rates at all the temperatures. The dependence of  $P_0$  on the molecular weight is higher than that of  $\eta$ .

### End Correction Coefficient

Figure 14 shows the variations, with the apparent shear rate  $\dot{\gamma}'_w$ , of the end correction coefficient  $\nu$  which was obtained as the intercept of the  $L/R$ -axis in the Bagley plot. Although, as a large tendency,  $\nu$  increases with increasing shear rate,  $\nu$  of HPC-H shows maxima at high temperatures. The shear rate at which  $\nu$  shows the maximum increases as the temperature increases.  $\nu$  changes in a complicated manner with temperature. Compared to general thermoplastic resins, a characteristic matter is that  $\nu$  of HPC is very high. There are cases for HPC-H and HPC-M where the value of  $\nu$  exceeds 50. Suto et al.<sup>7,8</sup> reported that  $\nu$  of lyotropic HPC increased or decreased with shear rate in a complicated manner, depending on the solvent and the concentration, and that there were cases where  $\nu$  showed a value higher than 40. Generally, thermoplastic resins show the value of  $\nu$  lower than 20 and more often lower than 10 in a usual shear rate range.<sup>15,16</sup>

Figure 15 shows the temperature changes of  $\nu$ .  $\nu$  shows a maximum and the temperature at the maximum is 200–210°C for HPC-H, about 190°C for HPC-M, and 160–170°C for HPC-L and is higher as the molecular weight is increased. The temperature at which  $\nu$  shows a maximum almost agrees with the temperature at which the liquid crystalline/biphasic transition begins.

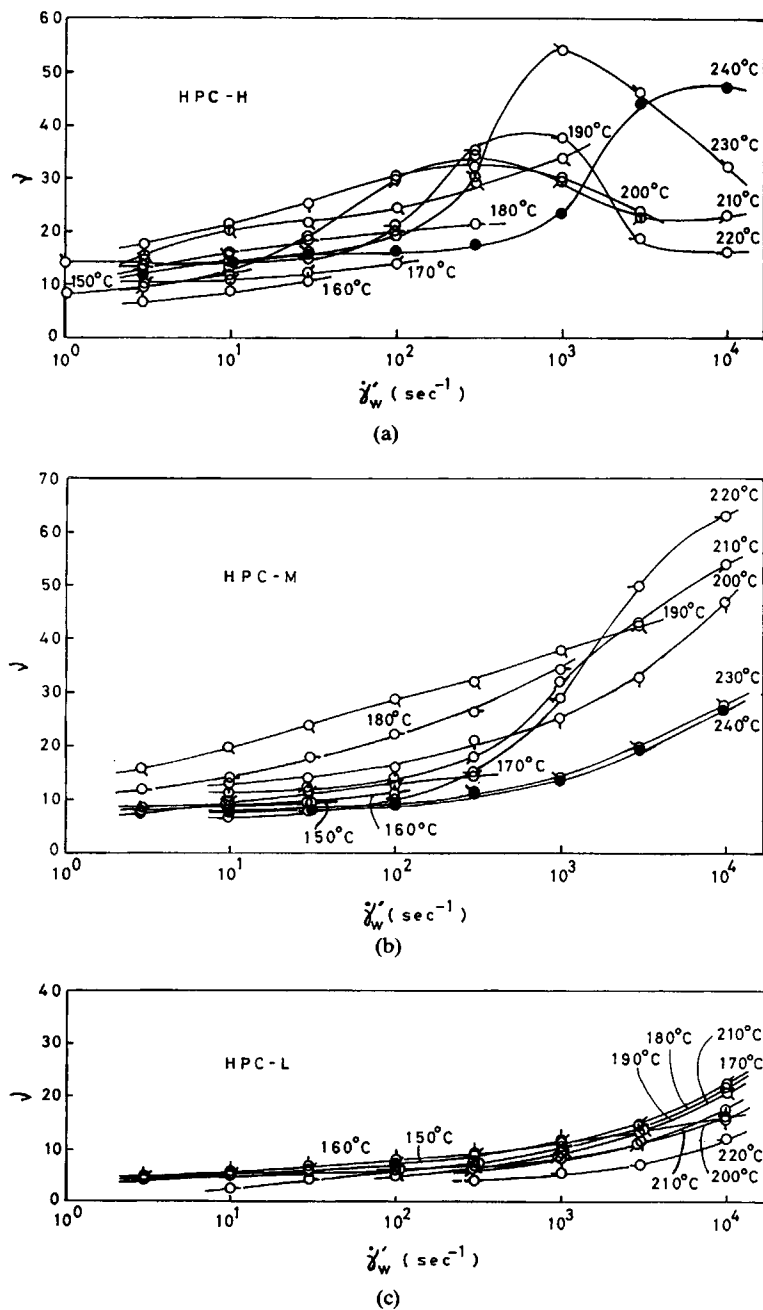


Fig. 14. Variations of end correction coefficient  $\gamma$  with apparent shear rate: (a) HPC-H; (b) HPC-M; (c) HPC-L.



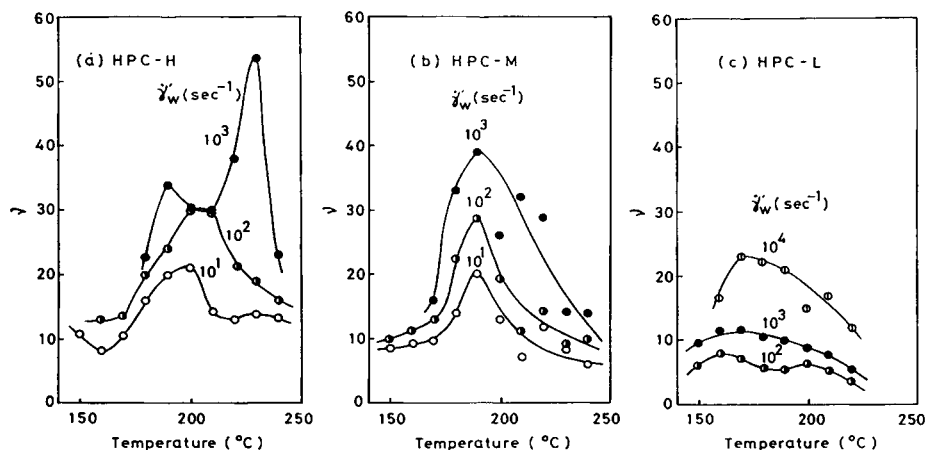


Fig. 15. Temperature changes of end correction coefficient  $\nu$ : (a) HPC-H; (b) HPC-M; (c) HPC-L.

Figure 16 shows a comparison of the temperature change of  $\nu$  among samples.  $\nu$  of HPC-H is nearly the same order as that of HPC-M. HPC-L shows a lower  $\nu$  value.

### Die Swell

Figure 17 shows the variations, with the apparent shear rate  $\dot{\gamma}_w$ , of the die swell ratio  $D/D_0$  measured with a die of  $L/R = 20$ . When other dies ( $L/R = 10$  and 4) were used, the absolute value of  $D/D_0$  increased with decreasing  $L/R$  and the relative tendencies were almost similar for all the dies. As a large

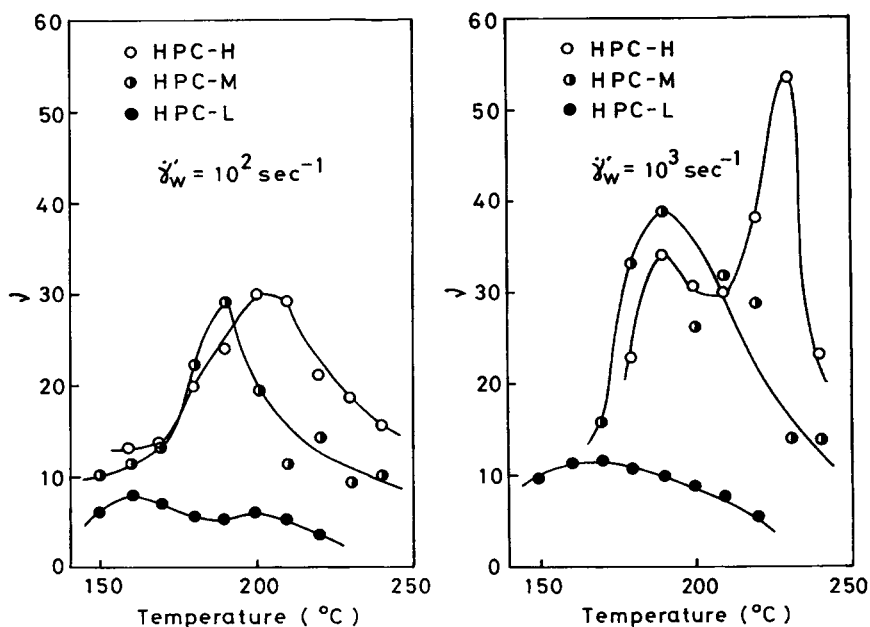


Fig. 16. Comparison of temperature change of end correction coefficient  $\nu$  among samples.

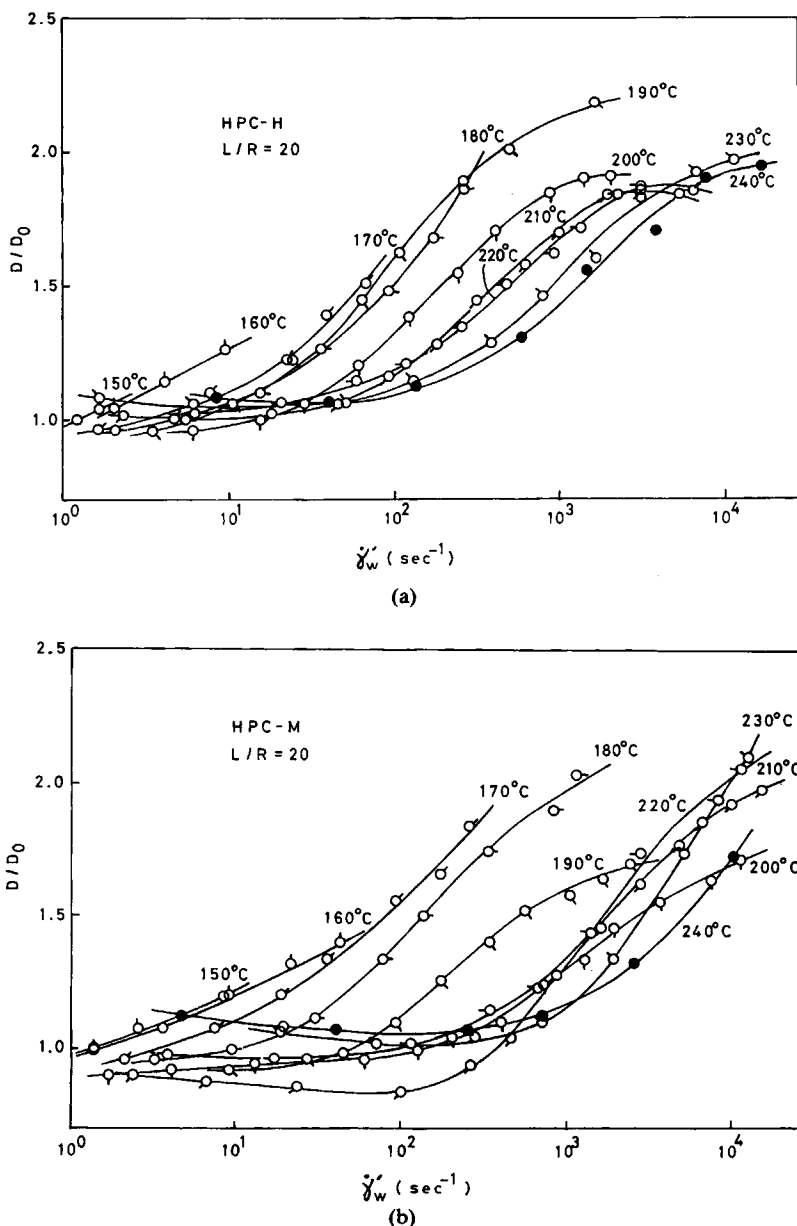


Fig. 17. Variations of die swell ratio  $D/D_0$  with apparent shear rate: (a) HPC-H; (b) HPC-M; (c) HPC-L.

tendency,  $D/D_0$  is nearly constant at low shear rates and increases with increasing shear rate. Clear maximum as in the case of lyotropic HPC<sup>8</sup> was not observed.  $D/D_0$  shows a value lower than unity at low shear rates in the temperature range of 180–220°C. The lowest value of  $D/D_0$  is 0.84 at  $\dot{\gamma}_w = 1.02 \times 10^2 \text{ s}^{-1}$  at 210°C for HPC-M. In such a case too,  $D/D_0$  is higher as  $L/R$  is smaller as shown in Figure 18. As a cause of too small die swell, the fact that the extrudate diameter  $D$  was measured after it was solidified is

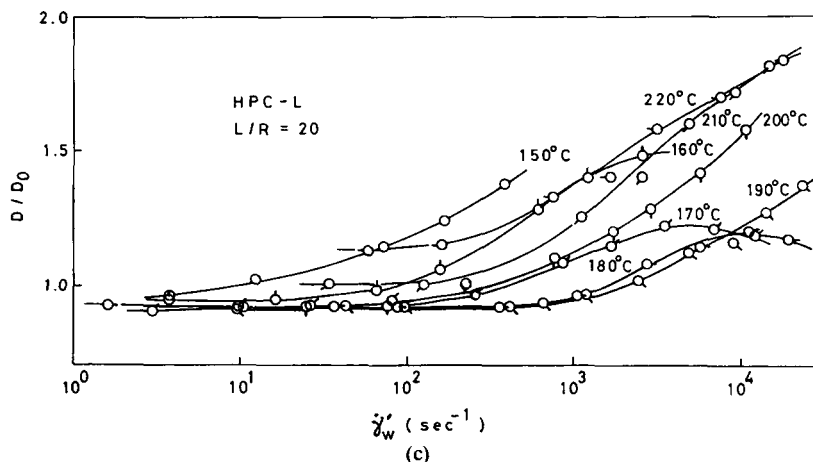
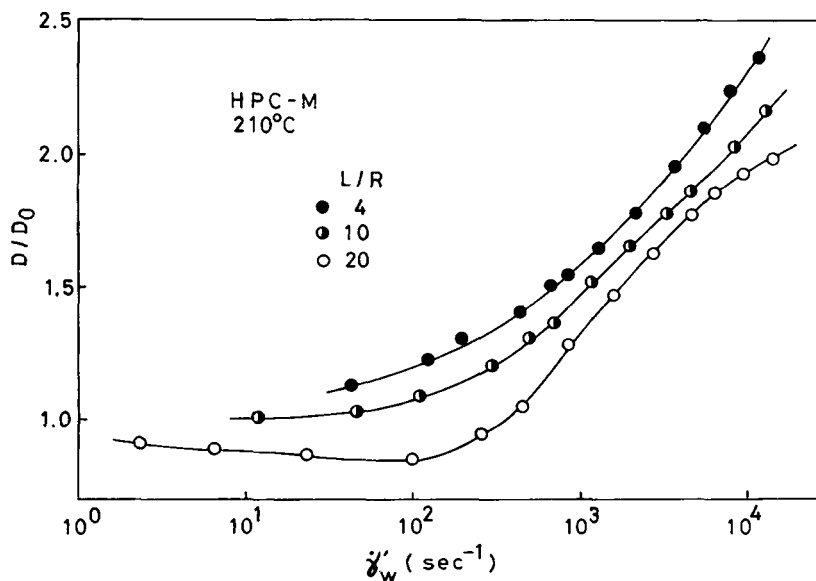


Fig. 17. (Continued from the previous page.)

considered. According to Samuels,<sup>17</sup> the density of HPC at room temperature is 1.17 g/cm<sup>3</sup> and the density at 170–230°C is 1.01 g/cm<sup>3</sup>. If  $D/D_0$  is corrected by the density,  $D/D_0$  at 170–230°C is 1.05 times that at room temperature. Therefore, if  $D/D_0$  at room temperature is lower than 0.95,  $D/D_0$  at 170–230°C is lower than unity. Many cases where  $D/D_0$  at room temperature was lower than 0.95 were observed in this experiment. In such cases, the diameter of the extrudate actually contracts after it passes through a die. Suto et al.<sup>4</sup> also reported a case where  $D/D_0$  of a thermotropic HPC was lower than unity. Similar results were also reported for thermotropic copolyesters.<sup>14, 18–20</sup>

Figure 19 shows the temperature changes of  $D/D_0$ . The lines are drawn faithfully to the points since the results obtained with other dies ( $L/R = 10$

Fig. 18. Dependence of die swell ratio  $D/D_0$  on die dimension.

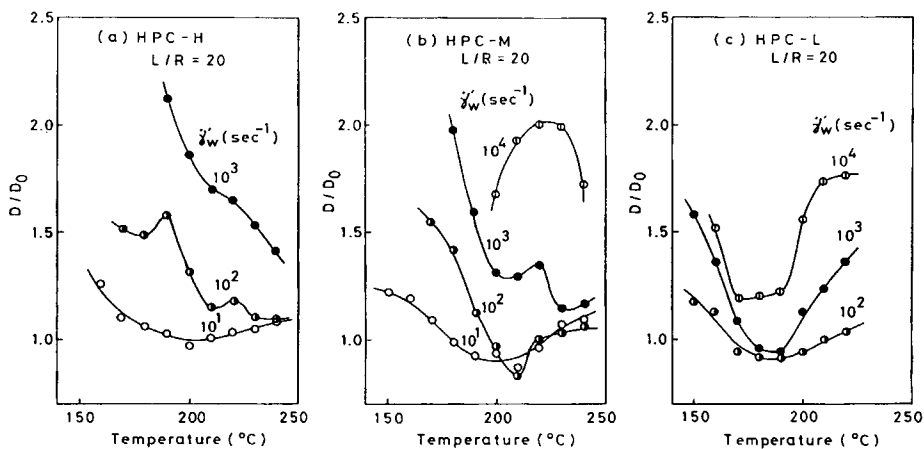


Fig. 19. Temperature changes of die swell ratio  $D/D_0$ : (a) HPC-H; (b) HPC-M; (c) HPC-L.

and 4) showed similar behaviors.  $D/D_0$  changes in a complicated manner, depending on the molecular weight and the shear rate. Suto et al.<sup>7,8</sup> reported that  $D/D_0$  of lyotropic HPC changed in a complicated manner depending on the solvent, the concentration, and the shear stress. In the case of thermotropic HPCs in this experiment, a thing common to three samples is that  $D/D_0$  shows a minimum lower than unity in the temperature range of 180–220°C at low shear rates.

Figure 20 shows a comparison of the temperature change of  $D/D_0$  among samples. As a large tendency,  $D/D_0$  is higher as the molecular weight is increased.

Suto et al.<sup>8</sup> reported that in the case of lyotropic HPCs the concentration dependence of the entrance pressure loss  $P_0$ , the end correction coefficient  $\nu$ , and the swell ratio  $D/D_0$  showed similar tendencies. However, in the case of

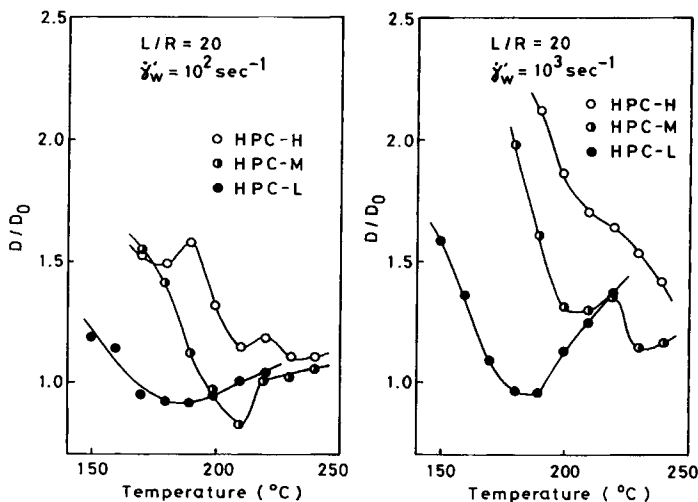


Fig. 20. Comparison of temperature change of die swell ratio  $D/D_0$  among samples.

thermotropic HPCs in this experiment, no similarity was observed in their temperature dependence.

### CONCLUSIONS

The influences of molecular weight, temperature, and shear rate on the capillary flow properties of thermotropic HPCs have been studied and the following conclusions have been obtained:

(i) The crystalline/liquid crystalline transition temperature and the temperatures at which the liquid crystalline/isotropic transition begins and ends are higher as the molecular weight is increased.

(ii) The flow curves show yield stresses and, contrary to general thermoplastic resins, the slope of  $\log(\text{viscosity})-\log(\text{shear rate})$  curve decreases with increasing shear rate. This tendency is more notable as the molecular weight is higher.

(iii) A minimum appears in the temperature change of the viscosity, which is caused by a balance between the decrease of the viscosity of the liquid crystalline phase with increasing temperature and the increase of the viscosity due to the transition from the liquid crystalline phase to the isotropic phase which has higher viscosity than the liquid crystalline phase at the temperature. The temperature at which the viscosity shows a minimum moves toward higher temperature with increasing shear rate. The moving rate is higher as the molecular weight is higher. This is because the degree of the molecular orientation in the isotropic phase increases and hence the viscosity difference between the liquid crystalline and the isotropic phases decreases with increasing shear rate and molecular weight. The viscosity is higher as the molecular weight is higher and, contrary to general thermoplastic resins, the molecular weight dependence of the viscosity increases with increasing shear rate.

(iv) The yield stress is higher as the molecular weight is higher and shows a minimum at 200–210°C.

(v) The molecular weight dependence of the entrance pressure loss is higher than that of the viscosity.

(vi) The end correction coefficient of thermotropic HPCs is much higher than that of general thermoplastic resins and there are cases where its value exceeds 50. The temperature change of the end correction coefficient shows a maximum and the temperature at the maximum increases as the molecular weight is increased. The temperature almost agrees with the liquid crystalline/biphasic transition temperature.

(vii) There are cases where the die swell ratio shows a value lower than unity in the temperature range of 180–220°C at low shear rates. The swell ratio is higher as the molecular weight is increased.

The author would like to thank Tokuyama Soda Co, Ltd., for permission to publish this paper.

### References

1. K. F. Wissbrun, *J. Rheol.*, **25**, 619 (1981).
2. T. Masuda and K. Fujiwara, *High Polym., Jpn.*, **36**, 106 (1987).
3. K. Shimamura, J. L. White, and J. F. Fellers, *J. Appl. Polym. Sci.*, **26**, 2165 (1981).
4. S. Suto, J. L. White, and J. F. Fellers, *Rheol. Acta*, **21**, 62 (1982).

5. J. Chen, J. L. White, and T. Kyu, *SPE Tech. Pap.*, 44th ANTEC, 723 (1986).
6. M. Horio, E. Kamei, and K. Matsunobu, *Nihon Reoraji Gakkaishi*, **16**, 27 (1988).
7. S. Suto, M. Ohshiro, R. Ito, and M. Karasawa, *Nihon Reoraji Gakkaishi*, **14**, 87 (1986).
8. S. Suto, M. Ohshiro, R. Ito, and M. Karasawa, *Polymer*, **28**, 23 (1987).
9. E. B. Bagley, *J. Appl. Phys.*, **28**, 624 (1957).
10. B. Z. Rabinowitsch, *Z. Physik, Chem. (Leipzig)*, **A145**, 1 (1929).
11. M. J. Seurin, A. ten Bosch, and P. Sixou, *Polym. Bull.*, **9**, 450 (1983).
12. S. Onogi and T. Asada, in *Rheology*, G. Astarita, G. Marrucci, and L. Nicolais, Eds., Plenum, New York, 1980, Vol. 1, p. 127-147, Paper Presented at Eighth International Congress on Rheology, Naples, 1980.
13. N. Casson, *Rheology of Dispersed Systems*, C. C. Mills, Ed., Pergamon, London, 1959, p. 84.
14. H. Sugiyama, D. N. Lewis, J. L. White, and J. F. Fellers, *J. Appl. Polym. Sci.*, **30**, 2329 (1985).
15. L. B. Ryder, *SPE J.*, 1305 (Dec. 1961).
16. T. Arai and H. Aoyama, *Trans. Soc. Rheol.*, **7**, 333 (1963).
17. R. J. Samuels, *J. Polym. Sci. A-2*, **7**, 1197 (1969).
18. R. E. Jerman and D. G. Baird, *J. Rheol.*, **25**, 275 (1981).
19. D. A. Simoff and R. S. Porter, *Mol. Cryst. Liq. Cryst.*, **110**, 1 (1984).
20. A. D. Gotsis and D. G. Baird, *J. Rheol.*, **29**, 539 (1985).

Received November 4, 1988

Accepted February 22, 1989